ARTICLE

ACS chemical biology

Synthetic Inositol Phosphoglycans Related to GPI Lack Insulin-Mimetic Activity

Marie-Lyn Hecht[†,‡,∥,⊥], Yu-Hsuan Tsai[†,‡], Xinyu Liu[∥,○], Christian Wolfrum[⊥,#], and Peter H. Seeberger[†,‡,∥,*]

[†]Department of Biomolecular Systems, Max Planck Institute of Colloids and Interfaces, Am Mühlenberg 1, 14476 Potsdam, Germany, [‡]Freie Universität Berlin, Arnimallee 22, 14195 Berlin, Germany, [∥]Laboratory of Organic Chemistry, Swiss Federal Institute of Technology (ETH) Zurich, 8093 Zurich, Switzerland, [⊥]Competence Center for Systems Physiology and Metabolic Diseases, Zurich, 8093 Zurich, Switzerland, and [#]Institute of Molecular Systems Biology, Swiss Federal Institute of Technology (ETH) Zurich, 8093 Zurich, Switzerland. [○]Current address: Department of Chemistry, University of Pittsburgh, 219 Parkman Avenue, Pittsburgh, PA 15260.

ABSTRACT Insulin signaling has been suggested, at least in part, to be affected by an insulin-mimetic species of low molecular weight. These inositol phosphoglycans (IPGs) are generated upon growth hormone/cytokine stimulation and control the activity of a multitude of insulin effector enzymes. The minimal structural requirements of IPGs for insulin-mimetic action have been debated. Two types of IPGs were suggested, and the IPG-A type resembles the core glycan of glycosylphosphatidylinositol (GPI)-anchors. In fact, purified GPI-anchors of lower eukaryotic origin have been shown to influence glucose homeostasis. To elucidate active IPGs, a collection of synthetic IPGs designed on the basis of previous reports of activity were tested for their insulin-mimetic activity. *In vitro* and *ex vivo* assays in rodent adipose tissue as well as *in vivo* analyses in mice were employed to test the synthetic IPGs. None of the IPGs we tested mimic insulin actions as determined by PKB/Akt phosphorylation and quantification of glucose transport and lipogenesis. Furthermore, none of the IPGs had any effect in *in vivo* insulin tolerance assays. In stark contrast to previous claims, we conclude that neither of the compounds tested is insulin-mimetic.

The peptide hormone insulin regulates glucose homeostasis by modulating the action of a multitude of metabolic enzymes in the liver, adipose tissue, and skeletal muscle. Upon insulin receptor activation and phosphorylation of the insulin-receptor substrates (IRSs), insulin signaling branches into several pathways leading to glucose uptake, lipogenesis, glycogen synthesis, glycolysis, and other anabolic processes. The existence of an alternative pathway that involves an insulin-mimetic species of low molecular weight was proposed more than 20 years ago (*1, 2*). Second messengers referred to as inositol phosphoglycans (IPGs) are generated in response to insulin (for a review see ref 3). The insulin-mimetic effect of IPGs has been demonstrated in adipocytes (*4*), hepatocytes (*5*), and muscle cells (*4*). In addition, IPGs are involved in mitogenic signaling *via* type I cytokine receptors (*6, 7*), suggesting a broader role of IPGs as second messengers in the hormone/cytokine signaling network. However, the mechanistic details of IPG action remain largely unknown. Considering the proposed insulin-mimetic activity, IPGs would be the basis for diabetes type 2 therapies. Type 2 diabetes is characterized by the resistance of peripheral tissues to insulin due to a combination of defects including impaired insulin signal transduction.

Analysis of isolated insulin-mimetic IPGs from insulin-sensitive mammalian tissue or lower eukaryotes revealed two structurally and functionally distinctive classes of IPGs (*8*). Type-A IPGs consist of *myo*-inositol and D-glucosamine, whereas type-P IPGs contain 3-*O*-methyl-D-*chiro*-inositol and D-galactosamine (*5, 9*). IPG-As mimic the lipogenic activity of insulin in adipose

***Corresponding author,**
seeberger@mpikg.mpg.de.

Received for review July 19, 2010
and accepted September 8, 2010.
Published online September 8, 2010
10.1021/cb1002152

tissue and inhibit cAMP-dependent protein kinase (*8*). IPG-Ps mimic the glycogenic effect of insulin on muscle and liver and stimulate pyruvate dehydrogenase phosphatase (*5, 8, 10*). While the composition of type-A IPGs implies a structural relationship to the glycosylphosphatidylinositol (GPI) glycolipids, the origin of IPG-P messengers is unclear. The similarity between IPG-A and GPI glycans is supported by the fact that antibodies raised against GPI-anchors crossreact with IPG preparations (*11*). Moreover, insulin-stimulated glycogen synthesis in K562 cells requires the biosynthesis of GPI anchors (*12*). GPI-anchored proteins are found in lipid rafts on virtually all eukaryotic cell surfaces (*13*). They are particularly abundant on the surface of protozoan parasites. GPIs anchor proteins to the outer leaflet of the plasma membrane or occur in free from. The GPI core structure consists of EtN-P-6-Man-α1,2-Man-α1,6-Man-α1,4-GlcN-α1,6-*myo*-D-inositol-1-P-lipid that can be decorated by many different species- and tissue-specific modifications (*14*). Lipolytically and proteolytically degraded GPI-anchored proteins from parasites (*15–18*) and yeast (*4, 19, 20*) have been shown to regulate glucose homeostasis in the rodent animal model. A number of active IPG-As carry a 1,2-cyclic phosphate at *myo*-inositol (*19, 21–24*). It has been suggested that IPG-As are generated by cleavage of GPI anchors through the action of a phospholipase C (PLC) (*25*). However, only indirect evidence for the existence of endogenous mammalian GPI-PLCs has been obtained by monitoring GPI-PLC action (*26, 27*). The gene for mammalian GPI-PLC has never been identified. The details of both generation of IPGs and IPG downstream signaling remain unclear.

The work presented here aims at clarifying the minimal active structure of GPI-derived insulin-mimetic IPGs using synthetic inositol phosphoglycans. Chemical synthesis, though challenging, provides analytically pure material in milligram quantities. Synthetic IPGs are an indispensable tool to shed light on a field where many contradicting reports can be found in the literature. The insulin-mimetic properties of synthetic IPGs have been investigated before (*21, 23, 24, 28–30*). Despite intensive efforts, there is no agreement on the composition of an active IPG-A molecule. An anionic GPI-type pseudotetrasaccharide (**IPG 3**, *vide infra*) that stimulates lipogenesis in rat adipocytes to 78% of maximal insulin response (MIR) has been described (*24*). Modest insulin-like activity of a GlcN-α1,6-*myo*-D-inositol-1,2-cyclicP pseudodisaccharide (**IPG 2**, *vide infra*) was also reported (*21, 22*). In contrast, the GPI core glycan pseudopentasaccharide without any modifications was shown not to have biological activity (*31*). The most comprehensive study published by Frick *et al.* (*23*) revealed a pseudohexasaccharide termed PIG 41 that displayed an insulin-mimetic activity of 90% MIR on lipogenesis in rat adipocytes (*23*). The structure of PIG 41-type molecules is related to GPI-glycans that bear different anionic modifications. However, the linkage between D-glucosamine and *myo*-inositol exhibits an unnatural β-configuration. Therefore, PIG 41-type molecules are not GPI-derived.

In this report, we investigated the insulin-mimetic potential of five GPI-type IPGs with diverse structural features. By analyzing an array of different compounds, we aimed at elucidating the structural requirements for IPGs to act as insulin-mimetics. We prepared type-A IPGs as they are structurally similar to GPI glycans and their source is evident. IPG-A activity can be monitored in rodent adipocytes (*21, 23, 24*). The synthetic GPI fragments differed in the lipidation state and the modification pattern and ranged from pseudodi- to pseudohexasaccharides. Two compounds that had been reported to exhibit insulin-mimetic activity were synthesized to serve as active controls. The ability of the IPGs to mimic insulin action in adipose tissue from mouse and rat was examined. PKB/Akt activation and glucose uptake were monitored in 3T3-L1 adipocytes, and PKB/Akt activation, glucose uptake, and lipogenesis were assessed in primary adipocytes from mice and rats. In addition, insulin tolerance tests were carried out in wild-type and diabetic mice. Our combined analysis conclusively shows that none of the tested IPGs mimic insulin action *in vitro* or *in vivo,* suggesting that the minimal active IPG structure remains elusive and new standards will be required for the study of insulin-mimetic IPGs.

RESULTS AND DISCUSSION

Synthesis of IPGs 1−5**.** To determine the structural features responsible for IPG insulin-mimetic activity, a small collection of structurally diverse inositol phosphoglycans (**IPGs 1−5**) was prepared (Figure 1). Pseudodisaccharide **IPG 2** (*21, 28*) and pseudotetrasaccharide **IPG 3** (*24*) with reported insulin-mimetic activity were resynthesized and used as controls. The chemical syntheses followed the routes depicted in Figure 2. **IPG 2** was prepared from known pseudodisaccharide **1** (*32*) in

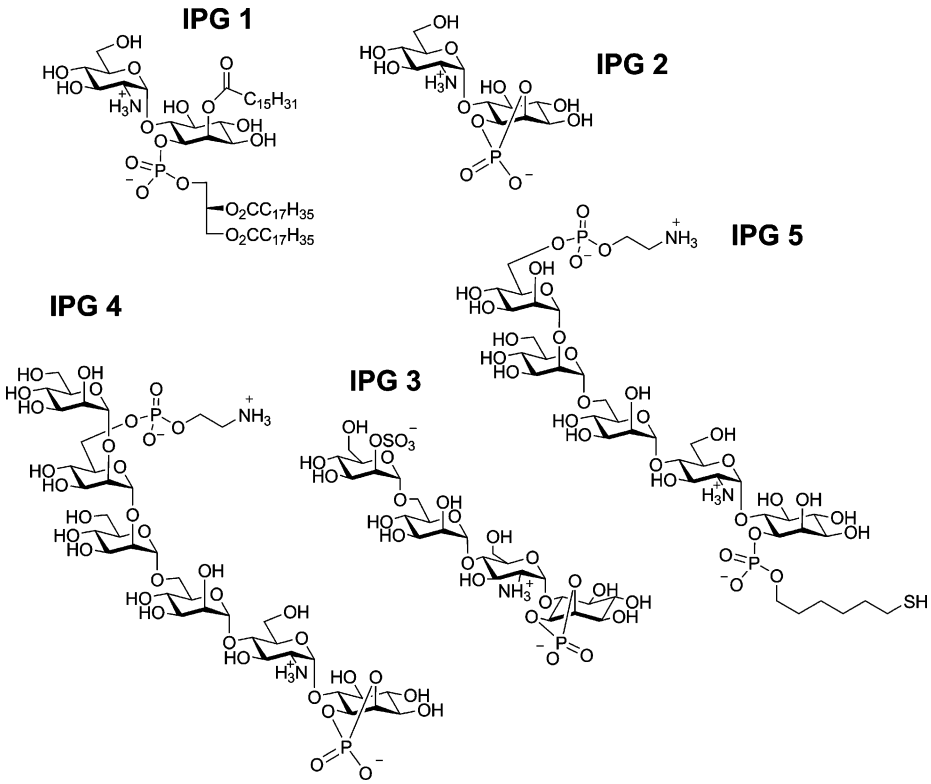

Figure 1. Overview of the synthetic inositol phosphoglycans (IPGs) tested in this study.

four steps *via* benzylation, acid hydrolysis of the isopropylidene, phosphorylation, and hydrogenation. **IPG 3** was constructed from key intermediates **1**, **4** (*32*), and **6** (*33*). Glycosidation of pseudodisaccharide **1** with mannosyl trichloroacetimidate **4**, saponification of the *O*-acetyl group, benzylation, and silyl ether cleavage provided pseudotrisaccharide **5**, which was glycosylated with mannosyl trichloroacetimidate **6** and hydrolysis of the isopropylidene group yielded pseudotetrasaccharide **7**. Phosphorylation of **7** followed by *O*-sulfation and global deprotection furnished **IPG 3**.

Additional IPGs used in this study include fully lipidated **IPG 1** (*34*) and GPI-like **IPG 4** and **IPG 5**. Fully lipidated **IPG 1** carries an ester-linked fatty acid at the C2 hydroxyl of inositol. Inositol acylation occurs during GPI biosynthesis and is usually reversed in mammals upon chain maturation. Nevertheless, there are inositol acylated GPI-modified proteins on the cell surface such as human erythrocyte acetylcholinesterase. The presence of this modification makes the anchor inherently resistant to the action of bacterial PI-PLC (*35*). Accordingly, no *myo*-inositol 1,2-cyclic phosphate, the long-lived intermediate of PLC (*36*), will be formed. The GPI-like glycans **IPG 4** and **IPG 5** that we had prepared previously were included (*37, 38*). An **IPG 4** conjugate had been successfully used for malaria vaccination in mice (*37*). Malaria is often accompanied by hypoglycaemia. This complication is thought to be induced by *Plasmodium falciparum* GPIs, one of the antigenic determinants of the malaria parasite (*39, 40*). Considering the protective effect of **IPG 4** against murine malaria and its close structural similarity to **PIG 41**-type IPGs, insulin-mimetic activity of **IPG 4** was conceivable. **IPG 5** was included because it is specifically recognized by anti-GPI antibodies in the serum of malaria-exposed individuals (*41*). Moreover, **IPG 5** carries an inositol with an unlipidated 1-phosphate in contrast to the 1,2-cyclic phosphate present in the other unlipidated compounds. We aimed at analyzing different phosphodiesters since the requirement and nature of the phosphate at the inositol to confer insulin-mimetic activity is still debated (*5, 22, 23*).

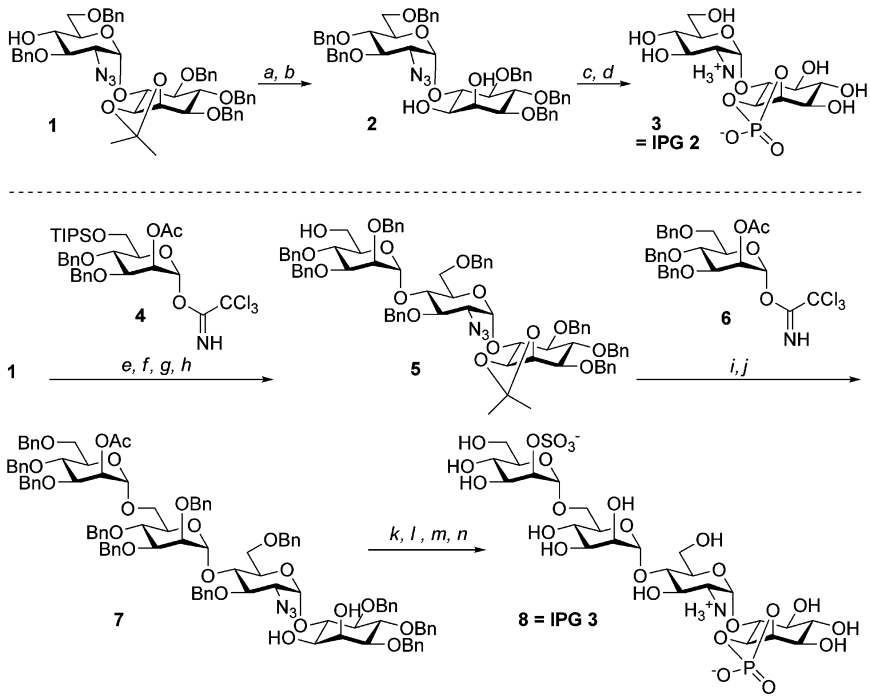

Figure 2. Synthesis of IPG 2 **and** IPG 3**. The reagents (*a*–*n*) were added at the indicated intermediates of glycan synthesis** 1–8**. (*a*) NaH, BnBr, DMF (73%); (*b*) AcCl, MeOH, DCM (92%); (*c*) $MeOP(O)Cl_2$, pyridine; (*d*) 20% $Pd(OH)_2/C$, H_2, THF, MeOH, H_2O (70%, 2 steps); (*e*)** 4**, TMSOTf, DCM (95%); (*f*) NaOMe, MeOH; (*g*) NaH, BnBr, DMF; (*h*) TBAF, THF (76%, 3 steps); (*i*)** 6**, TMSOTf, DCM (95%); (*j*) PTSA, MeOH (70%); (*k*) $MeOP(O)Cl_2$, pyridine; (*l*) NaOMe, MeOH; (*m*) $SO_3{\cdot}NEt_3$, DMF (57%, 3 steps); (*n*) 10% Pd/C, H_2, MeOH, H_2O (88%). NaH, sodium hydride; BnBr, benzyl bromide; DMF, *N*,*N*-dimethylformamide; AcCl, acetyl chloride; MeOH, methanol; DCM, dichloromethane; THF, tetrahydrofuran; TMSOTf, trimethylsilyl trifluoromethanesulfonate; NaOMe, sodium methoxide; TBAF, tetrabutylammonium fluoride; PTSA, *p*-toluenesulfonic acid; OBn, *O*-benzyl; TIPS, triisopropylsilyl; OAc, *O*-acetyl.**

PKB/Akt Activation in 3T3-L1 Cells and Primary Adipocytes. We sought to determine the insulin-mimetic potential of **IPGs 1–5** in adipose tissue since an insulin-mimetic effect in adipocytes had been reported previously for **IPG 2** and **IPG 3** (*21, 24*). Accordingly, we monitored the phosphorylation of PKB/Akt in 3T3-L1 adipocytes by Western blotting. The 3T3-L1 adipocytes are differentiated from fibroblasts of murine origin and have an adipocyte-like morphology. PKB/Akt is a major downstream target of PI-3 kinase. PI-3 kinase/PKB/Akt signaling controls most of the metabolic actions of insulin. Since IPG signaling has been shown to activate IRS-1 in rat diaphragms (*23*), we considered PKB/Akt a good target to analyze the insulin-mimetic activity of the IPG compounds. As depicted in Figure 3, panel A, no dose-dependent activation of PKB/Akt in 3T3-L1 adipocytes in response to **IPGs 1–5** was observed. As expected, PKB/Akt was activated by the addition of 100 nM insulin, and the insulin effect was inhibited by further addition of LY-294,00, which inhibits the generation of phosphatidylinositol 3-phosphate by blocking PI-3 kinase activity. To exclude that the negative result is due to reduced sensitivity of the 3T3-L1 cell line, we subjected **IPG 3** to the same assay with primary mouse adipocytes (Figure 3, panel B). Again, no insulin-mimetic activity was observed. Considering this result in combination with the fact that there is no precedence for the PKB/Akt activation approach in the literature, we concluded that PKB/Akt activation is not suitable for IPG screening.

Glucose Transport in 3T3-L1 and Primary Adipocytes. IPGs were previously shown to stimulate glucose uptake in primary adipocytes (*23*). Thus, we decided to quantify the effect of **IPGs 1–5** on glucose uptake in fat cells. Glucose transport is the immediate and most important consequence of insulin action and the rate-limiting step in glucose utilization. In this assay, cells were stimulated with increasing concentrations of **IPGs 1–5**, and transport of 2-deoxy-1-[^{3}H]-D-glucose and D-[1-^{14}C]-glucose, respectively, was monitored in 3T3-L1 (Figure 4, panel A) and primary murine adipocytes (Figure 4, panel B). None of the synthetic IPGs induced glucose transport. In contrast, insulin led to a significant increase of glucose uptake and the myotoxin cytochalasin B inhibited glucose transport. The glucose transport assay for **IPG 3** and **IPG 5** with rat adipocytes did not show stimulation either (Supplementary Figure 1). Co-stimulation of **IPG 3** and 1 nM insulin was tested to determine additive effects on glucose uptake. No signal increase resulted in primary rat adipocytes (Supplementary Figure 2). Taken together, these data imply that **IPGs 1–5** have no insulin-mimetic effect with regard to glucose transport in adipose tissue.

Lipogenesis in Primary Adipocytes. Next, we performed lipogenesis assays in mouse and rat primary adipocytes. This assay was the method of choice to analyze insulin-mimetic IPGs in previous studies by other

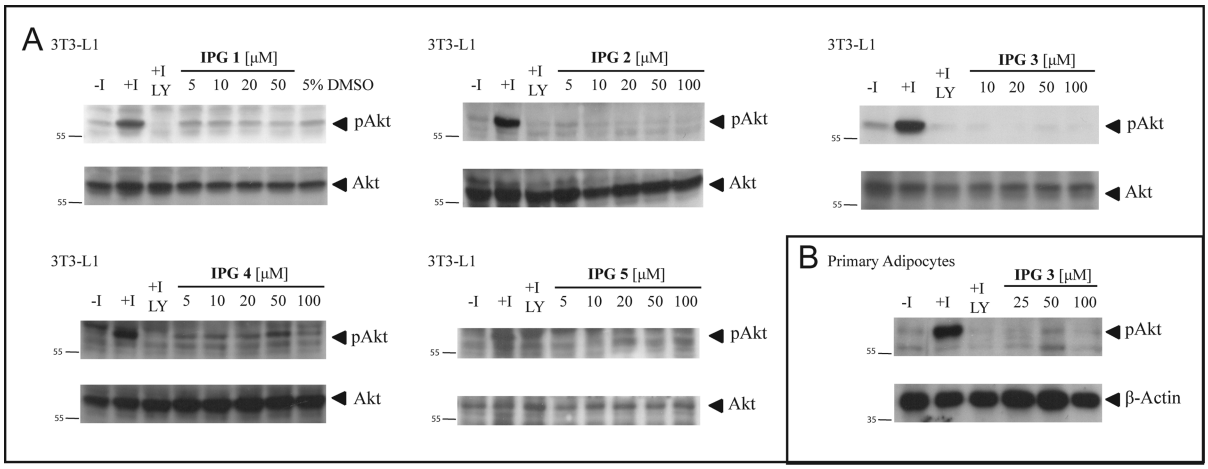

Figure 3. PKB/Akt activation assay. IPGs 1−5 **do not stimulate PKB/Akt phosphorylation. Cells were treated with insulin, LY-294,002 inhibitor and insulin, or IPG in varying concentrations and subjected to Western blot analysis. A) Activation assay in 3T3-L1 cells. −I: cells without prior treatment, +I: cells treated with 100 nM insulin, +I, LY: cells pretreated with 100 μM LY-294,002 and treated with 100 nM insulin, IPG [μM]: IPG in varying concentrations. B) Activation assay in primary murine adipocytes for** IPG 3**. The labeling is the same as in panel A. Western blot antibody against serine-phosphorylated Akt and total Akt.**

laboratories (*21, 23, 24*). Insulin controls *de novo* lipogenesis in a dual way. First, the concentration of glycolytically produced acetyl-CoA, which is the source for fatty acid synthesis, is determined by the availability of glucose. Second, insulin causes dephosphorylation of acetyl-CoA-carboxylase (ACC), which catalyzes the first step of fatty acid synthesis. From the previous experiments we can exclude an influence of **IPGs 1−5** on glucose availability. However, IPGs might stimulate lipogenesis by activating ACC. To test this hypothesis, we stimulated primary adipocytes with the synthetic compounds and measured conversion of radiolabeled glucose into lipids. Stimulation with **IPGs 1−5** failed to increase lipogenesis (Figure 5). This result deviates from the reported insulin-mimetic activity for **IPG 2** (30−40% MIR) (*21*) and **IPG 3** (78% MIR) (*24*) with respect to lipogenesis in rat adipocytes. Use of **IPG 3** in rat adipocytes also failed to stimulate lipogenesis (Supplementary Figure 3). We also tried to reset lipogenesis in the cells to zero by incubation with 90 nM isoproterenol and subsequent washing steps prior to stimulation as suggested by d'Alarcao (personal communication). Under these conditions, however, neither IPG-induced nor insulin-induced lipogenesis occurred. The isoproterenol prestimulation was abandoned since this kind of treatment generates an unphysiological metabolic state in the cells and is not meaningful for the *in vivo* situation. In combination, these results indicate that **IPGs 1−5** lack insulin-mimetic activity in fat tissue *in vitro* and *ex vivo*.

Insulin Tolerance Test. To substantiate our findings, the whole-body effect of **IPG** administration was determined by *in vivo* insulin tolerance tests in wild-type and ob/ob mice. To this end, glucose clearance was measured after intraperitoneal injection of insulin and the **IPGs**, respectively. Wild-type animals were fasted for 8 h, and ob/ob animals were fasted for 16 h prior to the experiment. Wild-type mice injected with insulin displayed gradually dropping glucose levels reaching a trough after 90 min. In contrast, synthetic **IPGs 1−5** did not alter blood glucose concentration significantly (Figure 6, panel A). The fluctuations observed in the glucose concentration curves are explained by stress-induced glucose release. In addition we performed insulin tolerance tests in ob/ob mice because purified IPG-As have been shown to induce hypoglycaemia in different diabetic mouse models including ob/ob mice (*42*). Over a period of 8 h none of **IPGs 1−5** decreased glucose levels (Figure 6, panel B). Although **IPGs 2−5** are assumed to be reasonably stable, we cannot exclude phosphodiester hydrolysis in **IPG 1** by GPI-PLD activity in the serum. Taken together, our data clearly demonstrate that **IPGs 1−5** exhibit no insulin-mimetic activity.

Discussion. In this comprehensive study we investigated the insulin-mimetic potential of five synthetic GPI-type inositol phosphoglycans in mouse and rat *in vitro*

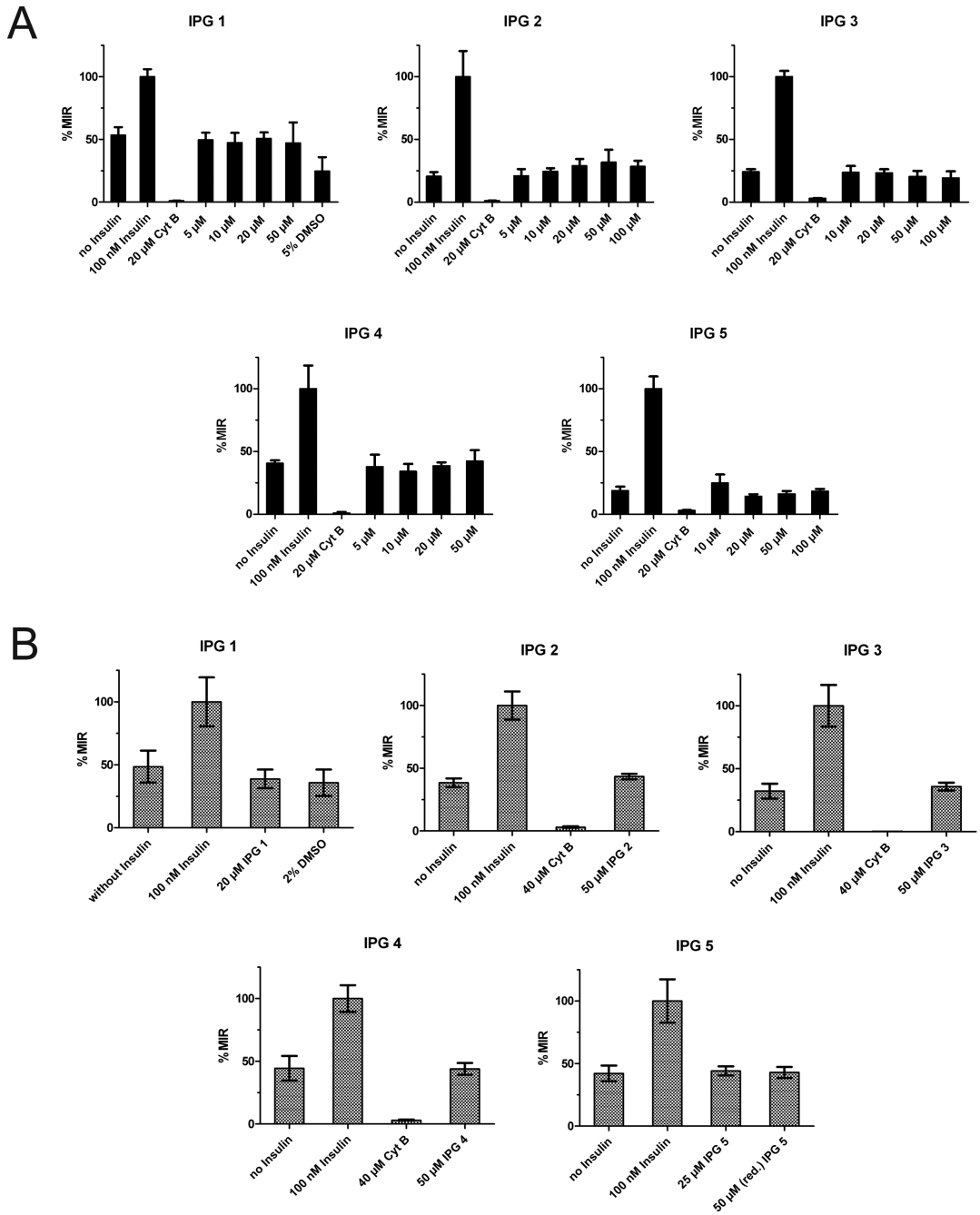

Figure 4. Glucose transport in (A) 3T3-L1 adipocytes and (B) primary adipocytes. IPGs 1−5 **have no effect on glucose transport in adipocytes. Cells were stimulated with 100 nM insulin, 20 μM cytochalasin B (Cyt B), or varying concentrations of** IPGs 1−5**. Stimulation of radiolabeled glucose uptake into cells was measured by liquid scintillation. Glucose transport is expressed relative to the maximal insulin response (%MIR). Each value represents the mean of at least three independent experiments ± SD.**

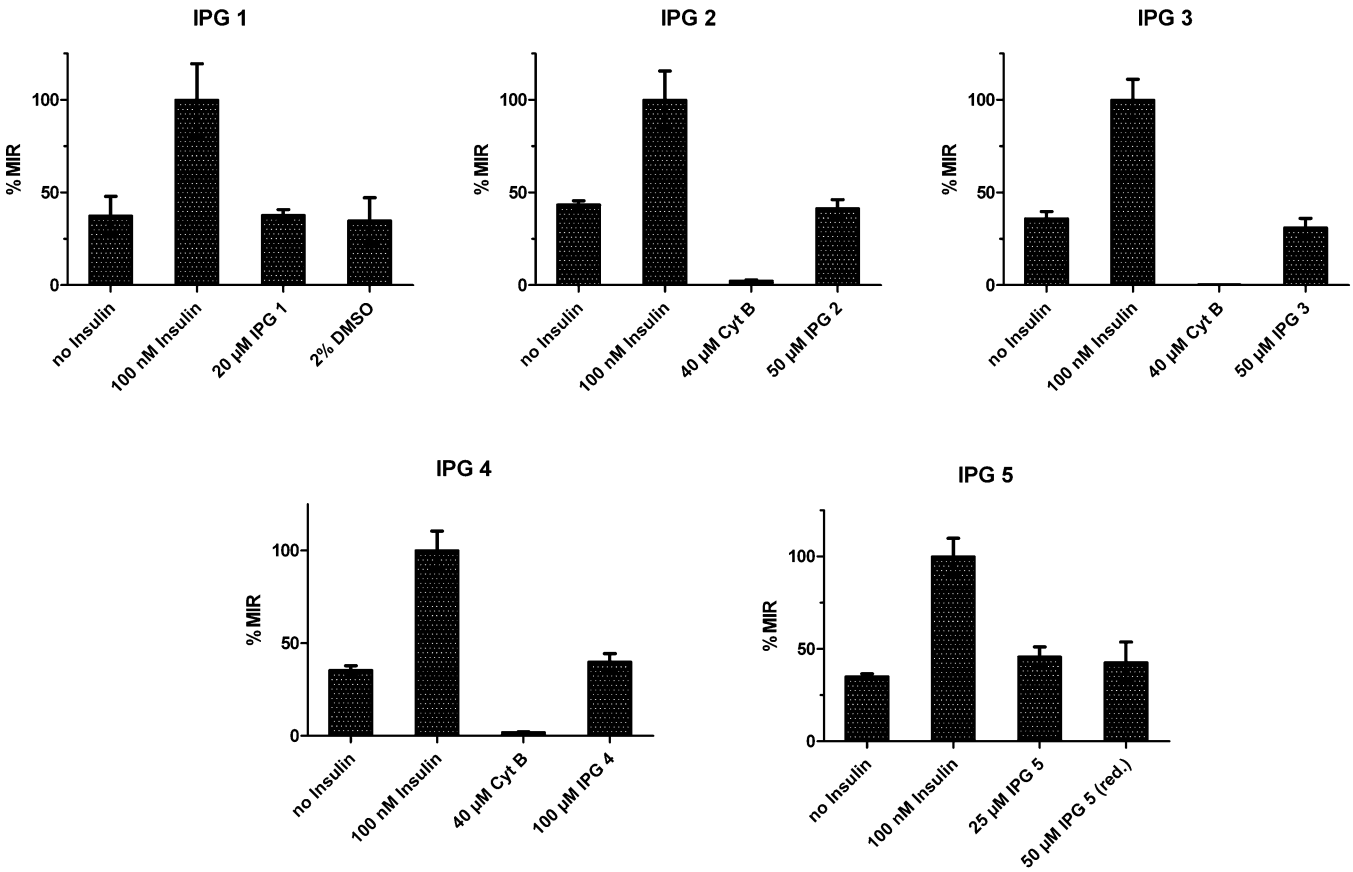

Figure 5. Lipogenesis in primary murine adipocytes. IPGs 1−5 **have no effect on lipogenesis in primary adipocytes. Cells were stimulated with 100 nM insulin, 20 μM cytochalasin B (Cyt B), or varying concentrations of** IPGs 1−5**. The conversion of ^{14}C-labeled glucose into toluene-extractable lipids was measured by liquid scintillation. Incorporation of heavy carbons into lipids is expressed relative to the maximal insulin response (%MIR). Each value represents the mean of at least three independent experiments ± SD.**

and *in vivo*. The synthetic IPG set analyzed included two compounds, **IPG 2** and **IPG 3**, that had previously been attributed insulin-mimetic activity in single assays (*21, 22, 24*). Our approach included two *in vitro* assays, three *ex vivo* assays and two *in vivo* tests. PKB/Akt activation and glucose transport were measured in 3T3-L1 and primary murine adipocytes, lipogenesis was analyzed in primary adipocytes from mouse and rat, and insulin tolerance tests were performed in wild-type and obese mice. Our data reveal that none of the compounds we tested is capable of inducing insulin effector functions in adipose tissue.

Previous studies have identified two different types of active IPGs. IPGs type-A are structurally related to GPI-anchors although the configuration of the linkage between D-glucosamine and *myo*-inositol is debated (*31*). Type-P IPGs, the other class of IPGs comprising D-galactosamine and 3-*O*-methyl-D-*chiro*-inositol, were not considered in this study. We chose to investigate GPI-type synthetic inositol phosphoglycans because (i) purified GPI-anchors from lower eukaryotes have been shown to induce hypoglycaemia in wild-type (*16, 43*) and diabetic rodents (*18*) and to mimic insulin actions in adipocytes, hepatocytes, and muscle cells (*4, 15, 17, 19*); (ii) antibodies raised against the GPI core glycan inhibit insulin action in BC3H1 cells (*11*); (iii) hypoglycaemia is a commonly observed condition of patients infected with the notoriously GPI-rich malaria parasite *P. falciparum* (*44*) and mice challenged with the murine malaria parasite *P. yoelli* (*45, 46*); and (iv) synthetic GPI-like core glycan and fragments thereof carrying anionic modifications have been shown to mimic insulin action

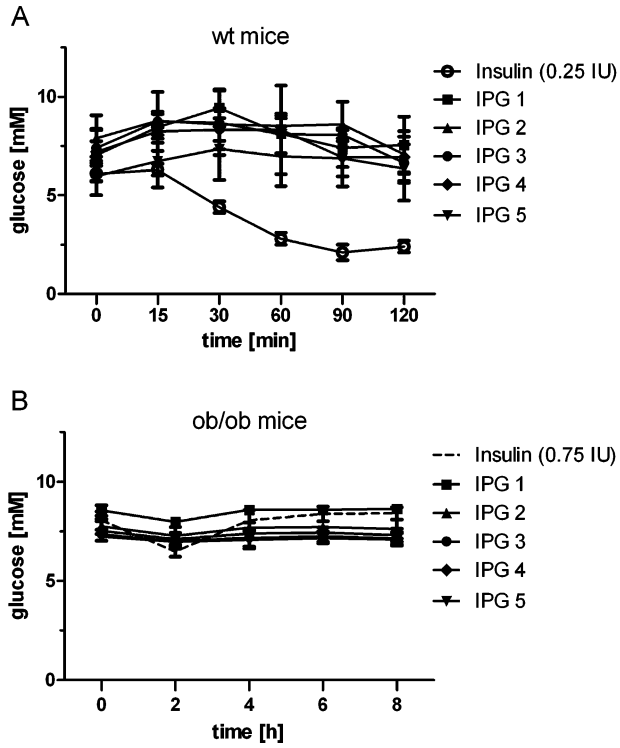

Figure 6. Insulin tolerance tests. A) IPGs 1−5 **do not lower glucose concentration in wild-type mice. Fasted C57BL/6 mice were injected with 0.25 IU insulin and 0.14 μmol kg^{-1} of** IPGs 1−5**, respectively. B)** IPGs 1−5 **do not lower glucose concentration in ob/ob mice. Fasted C57BL/6 ob/ob mice were injected with 0.75 IU insulin and 0.07 μmol kg^{-1} of** IPGs 1−5**, respectively. Glucose concentration was measured from blood taken from the tail vein at the indicated time points. Each value represents the mean of four independent experiments ± SD.**

in vitro (*21, 23, 24*). We are aware of the fact that the unmodified GPI core glycan has been shown not to be insulin-mimetic (*31*). It was suggested from other reports, however, that the presence of anionic modifications is crucial for bioactivity (*23, 24*).

The results presented here are in stark contrast to previous reports. Plourde *et al.* claimed an insulin-mimetic activity of **IPG 2** of 30−40% MIR in lipogenesis of rat adipocytes (*21*). Chakraborty *et al.* reported an insulin-mimetic activity of **IPG 3** of 78% MIR in lipogenesis in rat adipocytes (*24*). However, the two reports both present only one *ex vivo* assay. In contrast to these studies, we have conducted a thorough biological investigation, and our results show no significant, dose-dependent insulin-mimetic activity of **IPG 2** or **IPG 3**. It is conceivable that the compounds that were tested are not identical. We confirmed the structure of the synthetic molecules by nuclear magnetic resonance spectroscopy and mass spectrometry. In the case of **IPG 3**, we noted minor deviations in the ^{1}H NMR spectrum compared with published data (*24*). The authors confirmed an error in their reported ^{1}H NMR data that they intend to correct. For **IPG 2** the NMR spectra are in good agreement with the published data of Martín-Lomas and co-workers (*22*). Whereas Marc d'Alarcao and co-workers (*21*) reported a doublet at 19.9 ppm in the ^{31}P NMR, in our case a singlet at 16.4 ppm was observed (17.7 ppm reported by Martín-Lomas and co-workers). We believe that we prepared the correct molecule since the chemical shift of the cyclic phosphate is around 16 ppm in comparable structures (*24, 37*). Minor variations in the range of 1−2 ppm caused by differences in the NMR instruments are plausible, yet deviations in the range of 2−3 ppm are rather unlikely.

Our data are substantiated by different assays in different rodent animal models. All test systems were sensitive to insulin. Variations in the efficiency of insulin stimulation are normal and can be explained by small deviations in the experimental conditions. Standard protocols for adipocyte isolation were used. In order to economize animals, a mixture of visceral (epididymal) and subcutaneous fat was isolated. Pure epididymal fat might have been more responsive to insulin and presumably the IPGs, but the stimulation achieved with our protocol was sufficiently high to assess significant insulin-mimetic activity. Moreover, highly sensitive Western blot analysis did not reveal any activation of insulin signaling either. Degradation of the insulin or putative IPG receptor by trypsin in the collagenase preparation can be excluded since addition of trypsin inhibitor I to the digest of fat tissue did not alter the responsiveness of the cells (data not shown). In addition, insulin responsiveness of the adipocytes indicates that the insulin receptor and thus the cell surface proteins in general are intact and not affected by other protease contaminations. The *in vivo* studies were conducted similar to Elased *et al.* (*42*), who suggested an effect of purified IPG-A on serum glucose concentration in different diabetic mouse models. Serum-stability of the administered IPGs was not investigated. Ester hydrolysis of **IPG 1** is likely given the presence of GPI-PLD phosphodiesterases in the murine plasma (*47*). For the unlipidated GPI-derived glycans, *i.e.*, **IPGs 2−5**, it can be assumed

from reference studies that the half-life is sufficiently long to mediate effector functions.

Our results strongly support the notion that GPI-derived inositol phosphoglycans lack insulin-mimetic activity. Even **IPG 4**, which is structurally similar to the PIG 41-type pseudohexasaccharides presented by Müller (*23*) except for the α-glycosidic linkage connecting D-glucosamine to D-*myo*-inositol and the nature and the exact distribution of anionic modifications at the nonreducing end, is not an insulin-mimetic. We did not synthesize PIG 41 since the β-configuration of D-glucosamine has never been described in GPI-glycans (for reviews on GPI-anchors see ref 48) except by Müller (*20*). The origin of such a glycan species remains elusive. We conceive three possible explanations that could account for the lack of observed insulin-mimetic activity of the synthetic **IPGs 1−5**: (i) cleaved GPI molecules are further modified *in situ* before taking action; (ii) a completely novel type of GPI-anchors exists that has never been described; or (iii) the entire concept of insulin-mimetic inositol phosphoglycans is flawed and a different, yet unknown, molecular species was copurified in the numerous reports about isolated, bioactive IPGs.

The structure−activity relationship of insulin-mimetic inositol phosphoglycans remains elusive. In fact, there are partly conflicting data, and in many cases the biological testing is rudimentary and/or the molecules are poorly characterized. Some published results remained irreproducible (*21, 24*), yet without a minimal active structure the field cannot progress. All of the molecules tested have to be characterized thoroughly even if they are known, and biological results have to be cross-validated with multiple assays. Although *in vitro* experiments can be useful in analyzing IPGs and investigating the corresponding signaling pathway, only *in vivo* experiments can finally give information on whether a certain substance can be classified as an insulin-mimetic. After all, insulin is a systemic player that has a clear-cut effect: lowering glucose levels after food intake. The ultimate test for any potential insulin-mimetic agent has to be an *in vivo* experiment that assesses the ability of this substance to lower blood glucose concentration.

Signaling *via* GPI-derived IPGs has been suggested to modulate insulin signaling. An alternative pathway for insulin signaling could have implications on future diabetes type 2 therapies. However, there is still a long way to go. It is unclear how IPGs are composed and activated. Although many studies point toward the fact that IPGs are generated by insulin-induced cleavage of GPI-anchors, the details of this mechanism remain elusive. Questions concerning the topology of IPG signaling remain open. Müller and co-workers showed that IPGs bind to a 115 kDa protein on the outer leaflet of the plasma membrane (*49*), and d'Alarcao and co-workers demonstrated that fluorescently labeled IPGs exert their function from the outside of the cell (*29*). In contrast, IPGs have shown to regulate various intracellular enzymes in cell-free systems (*10, 50–52*). Along the same lines, there is no consensus about the identity of the IPG receptor. With sufficient quantities of a potent insulin-mimetic IPG in hand these pending questions could be addressed. Ultimately, advances in the field could provide novel means to defeat diabetes type 2, which has become a burden to human health around the globe.

METHODS

General. Unless otherwise specified, chemicals were purchased from Sigma-Aldrich. Gibco-DMEM (containing GlutaMAX I, 4500 mg L^{-1} glucose and 110 mg L^{-1} sodium pyruvate), Gibco Penicillin-streptomycin (10,000 U mL^{-1}) and Gibco Trypsin-EDTA (0.25%) solutions were purchased from Invitrogen. Acrylamide 4K-solution (30%) Mix 37.5:1 was purchased from AppliChem. Ammonium persulfate, *N*,*N*,*N*′,*N*′-tetramethylethylenediamine (TEMED), sodium dodecyl sulfate ultraPURE SDS, glycine ultra, BSA, and methanol were obtained from Fluka. Tris(hydroxymethyl)aminoethane (Tris) was purchased from Acros Organics. pAkt (Ser^{473}) and Akt antibodies were purchased from Santa Cruz Biotechnology. Anti-rabbit horseradish peroxidase conjugated antibody from donkey was obtained from Amersham Biosciences. Protease inhibitor cocktail Complete, EDTA-free was purchased from Roche. 2-Deoxy-1-[^{3}H]-D-glucose and [1-^{14}C]-D-glucose were purchased from PerkinElmer. **IPG 1** was dissolved in DMSO, and **IPGs 2−5** were dissolved in water. **IPG 5** was reduced by adding equimolar amounts of tris(2-carboxyethyl)phosphine (TCEP) prior to the experiment.

Synthesis of IPGs. IPG 1, **IPG 4**, and **IPG 5** were prepared as reported (*34, 37, 38*). The syntheses of **IPG 2** and **IPG 3** are described in detail in the Supporting Information. The identity and purity of compounds were assessed by nuclear magnetic resonance (NMR) spectroscopy.

Cell Culture. 3T3-L1 fibroblasts were grown and differentiated into adipocytes, as previously described (*53, 54*). Cells were used for experiments 11−13 days after induction of differentiation. In a typical experiment, 3T3-L1 adipocytes were preincubated in DMEM containing 4500 mg L^{-1} glucose without serum for 18 h in a humidified atmosphere with 5% CO_2 at 37 °C. After preincubation, 3T3-L1 adipocytes were washed three times with phosphate buffered saline (PBS) buffer (4.3 mM $NaHPO_4$,

1.4 mM KH_2PO_4, pH 7.4, 137 mM NaCl, 2.7 mM KCl) and then used for the experiment.

Western Blotting in 3T3-L1 Adipocytes. Serum-starved 3T3-L1 adipocytes were incubated in 500 μL of medium containing insulin (100 nM), LY-294,002 hydrochloride (100 μM) and insulin, or varying concentrations of IPG, for 60 min at 37 °C. Cells were washed twice with 1 mL PBS, 500 μL of ice-cold lysis buffer (1% Triton100 in PBS containing protease and phosphatase inhibitors) was added, and cells were scraped from the wells and transferred to tubes. Cells were lysed by shaking for 45 min at 4 °C. Suspensions were centrifuged for 15 min at 14,000 rpm at 4 °C. Cytosolic proteins were precipitated by addition of 50 μL 100% (w/v) trichloroacetic acid (TCA). After 45 min of incubation on ice the samples were centrifuged for 15 min at 14,000 rpm at 4 °C, and the pellets were washed twice with ice-cold acetone and allowed to dry. Pellets were resuspended in Laemmli SDS sample buffer. Protein concentrations were determined by Bradford analysis and adjusted. Samples were subjected to SDS-PAGE and transferred to nitrocellulose membrane (GE Healthcare). Membranes were blocked with 5% (w/v) BSA in Tris buffered saline (TBS) buffer (0.025 M Tris/HCl, pH 7.4, 0.137 M NaCl and 0.0025 M KCl) containing 0.1% (v/v) Tween20 for 1 h at RT. Membranes were incubated with the primary antibody overnight at 4 °C, followed by HRP-conjugated secondary antibody for 1 h at RT. Proteins were visualized by enhanced chemiluminescence (ECL). Subsequently, membranes were incubated in stripping buffer (62.5 mM Tris/HCl, pH 6.8, 100 mM 2-mercaptoethanol and 2% SDS) for 15 min at 50 °C and reprobed with primary and secondary antibody.

Glucose Transport in 3T3-L1 Adipocytes. Serum-starved 3T3-L1 adipocytes were incubated in 300 μL of Krebs-Ringer bicarbonate/HEPES (KRBH) buffer (30 mM HEPES, pH 7.4, 120 mM NaCl, 1 mM $MgSO_4$, 0.75 mM $CaCl_2$, 4 mM KH_2PO_4, 10 mM $NaHCO_3$) for 80 min at 37 °C. Insulin (100 nM), cytochalasin B (20 μM), or varying concentrations of IPG were added for 30 min. Glucose transport was initiated by the addition of 100 μL of KRBH containing 0.125 μCi of 2-deoxy-1-[^{3}H]-D-glucose for 4 min at 37 °C. After 4 min the transport was terminated by placing the cells on ice and removal of the supernatant. Wells were washed three times with ice-cold PBS. Cells were lysed by addition of 200 μL of lysis buffer (1% Triton100, 0.1% SDS in PBS) for 40 min at 4 °C, while shaking. Lysates were transferred to scintillation vials and mixed with 5 mL of toluene-based scintillation cocktail. ^{3}H concentrations were determined by liquid scintillation spectroscopy.

Animal Models. Animal experiments were performed with male wild-type or ob/ob C57BL/6 mice and male Sprague–Dawley rats, respectively. Animals were maintained on a 12-h light/dark cycle. All animal experiments were approved by the Veterinary Office in Zurich (Switzerland) or the Landesamt für Gesundheit and Soziales, LAGeSo, in Berlin (Germany).

Isolation of Primary Adipocytes. Subcutaneous and visceral fat pads were dissected from freshly sacrificed animals and kept in PBS until use, no longer than 0.5 h. Fat pads were cut into small pieces and incubated for 1 h in Krebs-Ringer Bicarbonate (KRB) buffer (purchased from Sigma, substituted with 2.5% BSA, 1% penicillin/streptomycin and 2 mg mL^{-1} collagenase type 2 from *Clostridium histolyticum*) at 37 °C, while shaking. The digested fat pads were filtered through a 350 μm^2 mesh and washed three times with KRBH buffer lacking glucose (30 mM HEPES, pH 7.4, 120 mM NaCl, 1 mM $MgSO_4$, 0.75 mM $CaCl_2$, 10 mM $NaHCO_3$, 4 mM KH_2PO, 1% BSA).

Western Blotting in Primary Adipocytes. Primary adipocytes were serum starved for 3 h and subsequently incubated in 500 μL of medium containing insulin (100 nM), LY-294,002 hydrochloride (100 μM), or varying concentrations of IPG, for 60 min at 37 °C. Cells were lysed by incubation in lysis buffer (50 mM Tris, pH 7.4, 150 mM NaCl, 5 mM EDTA, 0.1% SDS, protease and phosphatase inhibitors) for 30 min at 4 °C. Protein concentrations were determined by BCA analysis and adjusted. Suspensions were mixed with Laemmli SDS sample buffer and subjected to SDS-PAGE. Visualization of proteins was performed as described above.

Glucose Transport in Primary Adipocytes. Adipocyte suspension was mixed, diluted with KRBH containing 1% BSA, and distributed to a 24-well plate (300 μL per well). Insulin (100 nM), cytochalasin B (20 μM), or varying concentrations of IPG were added to the cells. After a preincubation period of 10 min at 37 °C, 50 μL of a 7 mM glucose solution containing 0.1 μCi D-[1-^{14}C]-glucose was added. The cells were incubated for 1 h at 37 °C, with mild shaking. An adipocyte solution of 200 μL was mixed with 300 μL of phthalate oil. The aqueous phase was separated from the cells by centrifugation for 1 min at 6000 × *g*. Adipocytes were washed with 100 μL PBS. Adipocytes were transferred to scintillation vials, and 4 mL of toluene-based scintillation liquid was added. β-decay was counted by liquid scintillation.

Lipogenesis in Primary Adipocytes. Adipocytes were incubated as described for glucose transport. After incubation, 150 μL of adipocyte suspension was mixed with 7 mL of toluene-based scintillation cocktail (2.5 g of 2,5-diphenyloxazole (PPO) and 0.15 g of 1,4-bis(5-phenyl-2-oxazolyl)benzene (POPOP) per 500 mL toluene) followed by vigorous mixing. The emulsion was centrifuged to expedite phase separation, 5 mL of the organic phase was removed, and β-decay was measured by liquid scintillation.

Insulin Tolerance Test. Wild-type mice, 10 weeks of age, were fasted for 8 h. Ob/ob mice, 9 weeks of age, were fasted for 16 h. Glucose levels were determined before injections with a Contour glucometer (Bayer) using blood from the tail vein. After i.p. injections of 0.25 U insulin kg^{-1} bodyweight and **IPGs 1−5** (0.14 μmol kg^{-1}), respectively, in C57BL/6 mice, glucose levels were monitored after 15, 30, 60, 90, and 120 min. After i.p. injections of 0.75 U insulin kg^{-1} bodyweight and **IPGs 1−5** (0.07 μmol kg^{-1}) in C57BL/6 ob/ob mice, glucose levels were monitored after 2, 4, 6, and 8 h.

Acknowledgment: This work was supported by ETH Zurich, the Max-Planck-Gesellschaft, and the German Academic Exchange Service DAAD (Doctoral Fellowship for Y.-H.T.). We thank Sara Schaufelberger for initial work in this project.

Supporting Information Available: This material is available free of charge *via* the Internet at http://pubs.acs.org.

REFERENCES

1. Larner, J., Galasko, G., Cheng, K., DePaoli-Roach, A. A., Huang, L., Daggy, P., and Kellogg, J. (1979) Generation by insulin of a chemical mediator that controls protein phosphorylation and dephosphorylation, *Science 206*, 1408–1410.
2. Saltiel, A. R., Fox, J. A., Sherline, P., and Cuatrecasas, P. (1986) Insulin-stimulated hydrolysis of a novel glycolipid generates modulators of cAMP phosphodiesterase, *Science 233*, 967–972.
3. Jones, D. R., and Varela-Nieto, I. (1998) The role of glycosylphosphatidylinositol in signal transduction, *Int. J. Biochem. Cell Biol. 30*, 313–326.
4. Kessler, A., Müller, G., Wied, S., Crecelius, A., and Eckel, J. (1998) Signalling pathways of an insulin-mimetic phosphoinositolglycan-peptide in muscle and adipose tissue, *Biochem. J. 330*, 277–286.
5. Larner, J., Price, J. D., Heimark, D., Smith, L., Rule, G., Piccariello, T., Fonteles, M. C., Pontes, C., Vale, D., and Huang, L. (2003) Isolation, structure, synthesis, and bioactivity of a novel putative insulin mediator. A galactosamine chiro-inositol pseudo-disaccharide Mn^{2+} chelate with insulin-like activity, *J. Med. Chem. 46*, 3283–3291.

6. Merida, I., Pratt, J. C., and Gaulton, G. N. (1990) Regulation of interleukin 2-dependent growth responses by glycosylphosphatidylinositol molecules, *Proc. Natl. Acad. Sci. U.S.A. 87*, 9421–9425.
7. Boudot, C., Kadri, Z., Petitfrere, E., Lambert, E., Chretien, S., Mayeux, P., Haye, B., and Billat, C. (2002) Phosphatidylinositol 3-kinase regulates glycosylphosphatidylinositol hydrolysis through PLC-γ_2 activation in erythropoietin-stimulated cells, *Cell Signalling 14*, 869–878.
8. Caro, H. N., Kunjara, S., Rademacher, T. W., León, Y., Jones, D. R., Avila, M. A., and Varela-Nieto, I. (1997) Isolation and partial characterisation of insulin-mimetic inositol phosphoglycans from human liver, *Biochem. Mol. Med. 61*, 214–228.
9. Larner, J., Huang, L. C., Schwartz, C. F., Oswald, A. S., Shen, T. Y., Kinter, M., Tang, G. Z., and Zeller, K. (1988) Rat liver insulin mediator which stimulates pyruvate dehydrogenase phosphate contains galactosamine and D-chiroinositol, *Biochem. Biophys. Res. Commun. 151*, 1416–1426.
10. Lilley, K., Zhang, C., Villar-Palasi, C., Larner, J., and Huang, L. (1992) Insulin mediator stimulation of pyruvate dehydrogenase phosphatases, *Arch. Biochem. Biophys. 296*, 170–174.
11. Romero, G., Gámez, G., Huang, L. C., Lilley, K., and Luttrell, L. (1990) Anti-inositolglycan antibodies selectively block some of the actions of insulin in intact BC_3H1 cells, *Proc. Natl. Acad. Sci. U.S.A. 87*, 1476–1480.
12. Lazar, D. F., Knez, J. J., Medof, M. E., Cuatrecasas, P., and Saltiel, A. R. (1994) Stimulation of glycogen synthesis by insulin in human erythroleukemia cells requires the synthesis of glycosylphosphatidylinositol, *Proc. Natl. Acad. Sci. U.S.A. 91*, 9665–9669.
13. Varki, A., Cummings, R. D., Esko, J. D., Freeze, H. H., Stanley, P., Bertozzi, C. R., Hart, G. W., and Etzler, M. E., Eds. (2009) *Essentials of Glycobiology*, 2nd ed., Cold Spring Harbor Laboratory Press, Cold Spring Harbor, NY.
14. Brewis, I. A., Ferguson, M. A., Mehlert, A., Turner, A. J., and Hooper, N. M. (1995) Structures of the glycosyl-phosphatidylinositol anchors of porcine and human renal membrane dipeptidase. Comprehensive structural studies on the porcine anchor and interspecies comparison of the glycan core structures, *J. Biol. Chem. 270*, 22946–22956.
15. Misek, D. E., and Saltiel, A. R. (1992) An inositol phosphate glycan derived from a *Trypanosoma brucei* glycosyl-phosphatidylinositol mimics some of the metabolic actions of insulin, *J. Biol. Chem. 267*, 16266–16273.
16. Schofield, L., and Hackett, F. (1993) Signal transduction in host cells by a glycosylphosphatidylinositol toxin of malaria parasites, *J. Exp. Med. 177*, 145–153.
17. Misek, D. E., and Saltiel, A. R. (1994) An inositol phosphate glycan derived from a *Trypanosoma brucei* glycosyl phosphatidylinositol promotes protein dephosphorylation in rat epididymal adipocytes, *Endocrinology 135* 1869–1876.
18. Elased, K. M., Gumaa, K. A., de Souza, J. B., Playfair, J. H., and Rademacher, T. W. (2004) Improvement of glucose homeostasis in obese diabetic db/db mice given *Plasmodium yoelii* glycosylphosphatidylinositols, *Metabolism 53*, 1048–1053.
19. Müller, G., Wied, S., Crecelius, A., Kessler, A., and Eckel, J. (1997) Phosphoinositolglycan-peptides from yeast potently induce metabolic insulin actions in isolated rat adipocytes, cardiomyocytes, and diaphragms, *Endocrinology 138*, 3459–3475.
20. Müller, G., Wied, S., Piossek, C., Bauer, A., Bauer, J., and Frick, W. (1998) Convergence and divergence of the signaling pathways for insulin and phosphoinositolglycans, *Mol. Med. 4*, 299–323.
21. Plourde, R., d'Alarcao, M., and Saltiel, A. R. (1992) Synthesis and characterization of an insulin-mimetic disaccharide, *J. Org. Chem. 57*, 2606–2610.
22. Zapata, A., Leòn, Y., Mato, J. M., Varela-Nieto, I., Penades, S., and Martín-Lomas, M. (1994) Synthesis and investigation of the possible insulin-like activity of 1D-4-*O*- and 1D-6-*O*-(2-amino-2-deoxy-α-D-glucopyranosyl)-*myo*-inositol 1-phosphate and 1D-6-*O*-(2-amino-2-deoxy-α-D-glucopyranosyl)-*myo*-inositol 1,2-(cyclic phosphate), *Carbohydr. Res. 264*, 21–31.
23. Frick, W., Bauer, A., Bauer, J., Wied, S., and Müller, G. (1998) Structure-activity relationship of synthetic phosphoinositolglycans mimicking metabolic insulin action, *Biochemistry 37*, 13421–13436.
24. Chakraborty, N., and d'Alarcao, M. (2005) An anionic inositol phosphate glycan pseudotetrasaccharide exhibits high insulin-mimetic activity in rat adipocytes, *Bioorg. Med. Chem. 13*, 6732–6741.
25. Saltiel, A. R., and Cuatrecasas, P. (1988) In search of a second messenger for insulin, *Am. J. Physiol. 255*, C1–11.
26. Park, S. W., Choi, K., Kim, I. C., Lee, H. H., Hooper, N. M., and Park, H. S. (2001) Endogenous glycosylphosphatidylinositol-specific phospholipase C releases renal dipeptidase from kidney proximal tubules *in vitro*, *Biochem. J. 353*, 339–344.
27. Müller, G., Schulz, A., Wied, S., and Frick, W. (2005) Regulation of lipid raft proteins by glimepiride- and insulin-induced glycosylphosphatidylinositol-specific phospholipase C in rat adipocytes, *Biochem. Pharmacol. 69*, 761–780.
28. Dietrich, H., Espinosa, J. F., Chiara, J. L., Jimenez-Barbero, J., Leon, Y., Varela-Nieto, I., Mato, J. M., Cano, F. H., Foces-Foces, C., and Martín-Lomas, M. (1999) Glycosyl inositol derivatives related to inositolphosphoglycan mediators: Synthesis, structure, and biological activity, *Chem.–Eur. J. 5*, 320–336.
29. Turner, D. I., Chakraborty, N., and d'Alarcao, M. (2005) A fluorescent inositol phosphate glycan stimulates lipogenesis in rat adipocytes by extracellular activation alone, *Bioorg. Med. Chem. Lett. 15*, 2023–2025.
30. Müller, G., Schulz, A., Dearey, E. A., Wetekam, E. M., Wied, S., and Frick, W. (2010) Synthetic phosphoinositolglycans regulate lipid metabolism between rat adipocytes via release of GPI-protein-harbouring adiposomes, *Arch. Physiol. Biochem. 116*, 97–115.
31. Martín-Lomas, M., Khiar, N., García, S., Koessler, J. L., Nieto, P. M., and Rademacher, T. W. (2000) Inositolphosphoglycan mediators structurally related to glycosyl phosphatidylinositol anchors: Synthesis, structure and biological activity, *Chem.–Eur. J. 6*, 3608–3621.
32. Hewitt, M. C., Snyder, D. A., and Seeberger, P. H. (2002) Rapid synthesis of a glycosylphosphatidylinositol-based malaria vaccine using automated solid-phase oligosaccharide synthesis, *J. Am. Chem. Soc. 124*, 13434–13436.
33. Liu, X., Stocker, B. L., and Seeberger, P. H. (2006) Total synthesis of phosphatidylinositol mannosides of *Mycobacterium tuberculosis*, *J. Am. Chem. Soc. 128*, 3638–3648.
34. Liu, X., and Seeberger, P. H. (2004) A Suzuki–Miyaura coupling mediated deprotection as key to the synthesis of a fully lipidated malarial GPI disaccharide, *Chem. Commun. (Cambridge)* 1708–1709.
35. Roberts, W. L., Myher, J. J., Kuksis, A., Low, M. G., and Rosenberry, T. L. (1988) Lipid analysis of the glycoinositol phospholipid membrane anchor of human erythrocyte acetylcholinesterase. Palmitoylation of inositol results in resistance to phosphatidylinositol-specific phospholipase C, *J. Biol. Chem. 263*, 18766–18775.
36. Hondal, R. J., Zhao, Z., Kravchuk, A. V., Liao, H., Riddle, S. R., Yue, X., Bruzik, K. S., and Tsai, M. D. (1998) Mechanism of phosphatidylinositol-specific phospholipase C: a unified view of the mechanism of catalysis, *Biochemistry 37*, 4568–4580.
37. Schofield, L., Hewitt, M. C., Evans, K., Siomos, M. A., and Seeberger, P. H. (2002) Synthetic GPI as a candidate anti-toxic vaccine in a model of malaria, *Nature 418*, 785–789.
38. Kwon, Y. U., Soucy, R. L., Snyder, D. A., and Seeberger, P. H. (2005) Assembly of a series of malarial glycosylphosphatidylinositol anchor oligosaccharides, *Chem.–Eur. J. 11*, 2493–2504.

39. Taylor, K., Carr, R., Playfair, J. H. L., and Saggerson, E. D. (1992) Malarial toxic antigens synergistically enhance insulin signaling, *FEBS Lett. 311*, 231–234.
40. Schofield, L., and Hackett, F. (1993) Signal transduction in host cells by a glycosylphosphatidylinositol toxin of malaria parasites, *J. Exp. Med. 177*, 145–153.
41. Kamena, F., Tamborrini, M., Liu, X. Y., Kwon, Y. U., Thompson, F., Pluschke, G., and Seeberger, P. H. (2008) Synthetic GPI array to study antitoxic malaria response, *Nat. Chem. Biol. 4*, 238–240.
42. Elased, K. M., Gumaa, K. A., de Souza, J. B., Rahmoune, H., Playfair, J. H., and Rademacher, T. W. (2001) Reversal of type 2 diabetes in mice by products of malaria parasites. II. Role of inositol phosphoglycans (IPGs), *Mol. Genet. Metab. 73*, 248–258.
43. Taylor, K., Bate, C. A., Carr, R. E., Butcher, G. A., Taverne, J., and Playfair, J. H. (1992) Phospholipid-containing toxic malaria antigens induce hypoglycaemia, *Clin. Exp. Immunol. 90*, 1–5.
44. World Health Organization, Division of Control of Tropical Diseases (1990) Severe and complicated malaria, *Trans. R. Soc. Trop. Med. Hyg. 84*, 1–65.
45. Elased, K., and Playfair, J. H. (1994) Hypoglycemia and hyperinsulinemia in rodent models of severe malaria infection, *Infect. Immun. 62*, 5157–5160.
46. Elased, K. M., de Souza, J. B., and Playfair, J. H. (2000) Reversal of type 2 diabetes in mice by products of malaria parasites: I. Effect of inactivated parasites, *Metabolism 49*, 937–941.
47. LeBoeuf, R. C., Caldwell, M., Guo, Y., Metz, C., Davitz, M. A., Olson, L. K., and Deeg, M. A. (1998) Mouse glycosylphosphatidylinositol-specific phospholipase D (*Gpld1*) characterization, *Mamm. Genome 9*, 710–714.
48. McConville, M. J., and Ferguson, M. A. (1993) The structure, biosynthesis and function of glycosylated phosphatidylinositols in the parasitic protozoa and higher eukaryotes, *Biochem. J. 294*, 305–324.
49. Müller, G., Hanekop, N., Kramer, W., Bandlow, W., and Frick, W. (2002) Interaction of phosphoinositolglycan(-peptides) with plasma membrane lipid rafts of rat adipocytes, *Arch. Biochem. Biophys. 408*, 17–32.
50. Saltiel, A. R. (1987) Insulin generates an enzyme modulator from hepatic plasma membranes: regulation of adenosine 3′,5′-monophosphate phosphodiesterase, pyruvate dehydrogenase, and adenylate cyclase, *Endocrinology 120*, 967–972.
51. Villalba, M., Kelly, K. L., and Mato, J. M. (1988) Inhibition of cyclic AMP-dependent protein kinase by the polar head group of an insulin-sensitive glycophospholipid, *Biochim. Biophys. Acta 968*, 69–76.
52. Huang, L. C., Heimark, D., Linko, J., Nolan, R., and Larner, J. (1999) A model phosphatase 2C → phosphatase 1 activation cascade via dual control of inhibitor-1 (INH-1) and DARPP-32 dephosphorylation by two inositol glycan putative insulin mediators from beef liver, *Biochem. Biophys. Res. Commun. 255*, 150–156.
53. Frost, S. C., and Lane, M. D. (1985) Evidence for the involvement of vicinal sulfhydryl groups in insulin-activated hexose transport by 3T3-L1 adipocytes, *J. Biol. Chem. 260*, 2646–2652.
54. Nelson, B. A., Robinson, K. A., and Buse, M. G. (2000) High glucose and glucosamine induce insulin resistance via different mechanisms in 3T3-L1 adipocytes, *Diabetes 49*, 981–991.